Temperature Indicators and Overtemperature Detection in Lithium-Ion Batteries based on Electrochemical Impedance Spectroscopy

Iñaki Lalinde[1,*], Alberto Berrueta[1], Adrian Soto[1], Joseba Arza[2], Pablo Sanchis[1] and Alfredo Ursúa[1]
[1]Institute of Smart Cities, Dept. of Electrical, Electronic and Communications Engineering,
Public University of Navarre (UPNA), Campus de Arrosadia, Pamplona, Spain
[2] Ingeteam R&D Europe, Polígono Parque Tecnológico, Zamudio, Spain
[*] Email: inaki.lalinde@unavarra.es

***Abstract*—Lithium-ion batteries are the leading technology for energy storage systems due to their attractive advantages. However, the safety of lithium-ion batteries is a major concern, as their operating conditions are limited in terms of temperature, voltage and state of charge. Therefore, it is important to monitor the conditions of lithium-ion batteries to guarantee safe operation. To this end, in the present work, we analyze electrochemical impedance spectroscopy (EIS) as a tool to estimate the temperature of batteries. Overtemperature abuse tests from 25 °C to 140 °C are performed at various states of charge, and EIS measurements are obtained during the tests. The influence of temperature on cell impedance at different frequencies is analyzed and new findings are revealed. The real part of the impedance is identified to be the best indicator for cell temperature estimation by EIS. In addition, the best frequency to achieve accurate temperature monitoring, avoiding disturbances produced by state of charge variations, is proposed based on experimental results. Finally, EIS is proven to be a reliable technique for overtemperature and thermal runaway detection.**

***Index Terms*—Lithium-ion batteries, safety, electrochemical impedance spectroscopy, impedance, temperature estimation**

I. Introduction

Lithium-ion batteries (LIBs) are widely used in portable electronic devices due to their attractive advantages, such as high energy and power density, long lifetime and low self-discharge. In addition, the need to integrate renewable energy and electric vehicles has driven their development, making them the leading technology compared to other energy storage systems [1]. However, safety issues related to LIBs are a serious concern. In particular, those resulting in thermal runaway (TR), which is the worst-case scenario that a LIB can face and leads to its sudden self-destruction [2]. Much effort and research is currently focused on the characterization [3] and modeling [4] of this phenomenon in order to understand its causes and propose safety measures to prevent it.

This work is part of the projects PID2019-111262RB-I00, funded by MCIN/AEI/10.13039/501100011033/, TED2021-132457B-I00, funded by MCIN/AEI/10.13039/501100011033/ and by the European Union NextGenerationEU/PRTR, STARDUST (774094), funded by European Union's Horizon 2020 research and innovation programme, HYBPLANT (0011-1411-2022-000039), funded by Government of Navarre, and has also been supported by MCIN/AEI/10.13039/501100011033/ and by European Social Fund under a PhD scholarship (grant PRE2020-095314).

LIBs are electrochemical systems consisting of different components, whose materials are sensitive to factors such as temperature, voltage or state of charge (SOC). Therefore, safe operating limits are defined to guarantee the suitable operation of LIBs. If these limits are exceeded, cells are exposed to undesired chemical reactions leading to fast degradation or malfunctioning, with effects such as capacity fade, resistance rise or efficiency reduction, or even severe damages with the potential to trigger a TR [5]. Fig. 1 represents the safe operating area of LIBs and the phenomena associated with the battery operation outside this safe area [4], [6].

To prevent LIBs from malfunctioning, it is essential to monitor that the state battery variables, such as temperature, voltage and SOC, are within safe conditions. Battery Management Systems (BMS) are responsible of this function and, if well designed, the risk of failure is significantly reduced [6]. However, unsafe conditions are unavoidable and new preventive measures are needed. Temperature is a major concern, as it significantly affects internal component materials and compromises the safety of LIBs. [7]. Fortunately, BMSs generally monitor the temperature within the battery. Nevertheless, most BMSs do not measure the temperature of each battery cell. Instead, the sensors are placed in strategical positions in order to reduce their number. In addition, the temperature distribution within the cell is not homogeneous so significant thermal gradients may occur inside LIBs [8]. As a result, the cell temperature may go outside the safe range not being detected by the sensors until it is too late. Therefore, faster and more reliable temperature monitoring is essential.

Electrochemical Impedance Spectroscopy (EIS) is a promising non-invasive technique that measures the cell impedance at different frequencies, providing valuable information about the properties of the cell internal components, interfacial phenomena and electrochemical reactions [9]. This directly relates to possible degradation inside the battery and is able to track the status of the battery such as the SOC or the State of Health (SOH) [10]. Although EIS measurements are usually performed with the cell at rest using specialized laboratory equipment, since impedance is a very good indicator of the internal state of the battery, methods are being proposed for

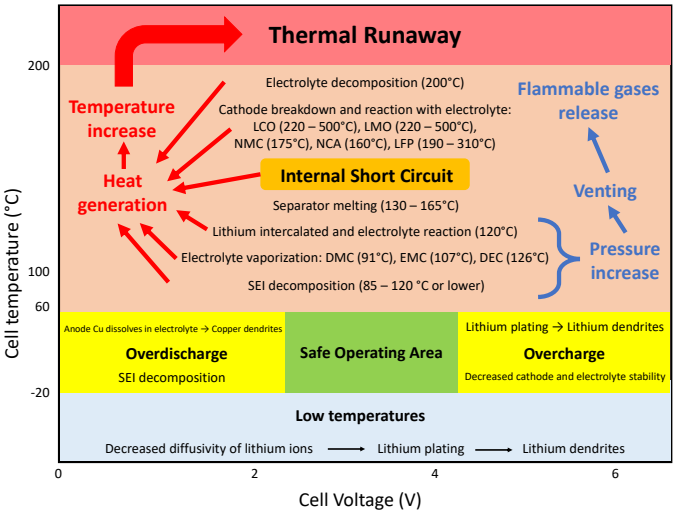

Fig. 1: Safe operating area of LIBs and phenomena associated to battery operation outside this safe area. Adapted from [3].

online application even when the battery is in operation [11].

Studies have confirmed the influence of temperature on cell impedance, and EIS has been identified as a suitable tool to monitor internal temperature. Srinivasan et al. [12] were the first to demonstrate the existence of an intrinsic relationship between cell internal temperature and the phase shift between an applied sinusoidal current and the resulting voltage in a range from –20 to 66 °C. In addition, they also propose impedance phase shift monitoring to detect cell venting and prevent thermal runaway [13]. Schmidt et al. [14] propose EIS as a sensorless online temperature measurement of LIBs and use the real part of cell impedance to monitor internal temperature. They characterize the cell impedance from –40 to 40 °C and find that SOC affects cell impedance, especially at low frequencies, which can reduce accuracy. For this reason, appropriate frequency selection can result in greater independence of the SOC. Zhu et al. [15] analyze the relationship between the phase shift and magnitude of cell impedance with temperature from –20 to 50 °C. They also demonstrate the influence of SOC and SOH on cell impedance and propose different frequencies for a better temperature estimation. Finally, Zappen et al. [16] perform EIS measurements during high-temperature abuse experiments that reveal a strong ability of impedance to detect battery degradation due to overtemperature. Therefore, EIS can address the problem of faster and more reliable temperature monitoring of LIBs, while reducing the number of sensors required.

In this work, we analyze and validate by means of experimental work the performance of EIS as a temperature estimator of LIBs to avoid unsafe conditions. For this purpose, EIS measurements are performed over a wide temperature range, from 25 °C to 140 °C on a commercial pouch cell. The influence of temperature on cell impedance is evaluated from the impedance variables and a comparison is made to determine which variable is the best for temperature estimation. Finally, based on the experimental results, the best frequency to achieve accurate temperature monitoring, avoiding disturbances caused by state of charge variations, is proposed.

II. Electrochemical Impedance Spectroscopy

EIS is a widely applied non-destructive method for characterization of LIBs from their impedance. The internal impedance of a battery is an important characteristic that has a direct effect on its operating voltage, rate capability and efficiency [17]. In addition, as mentioned above, EIS also provides valuable information on the properties of internal components and electrochemical reactions, enabling the monitoring of LIBs state. Therefore, its usefulness in estimation applications such as SOC, SOH or temperature is very promising.

EIS allows obtaining the complex impedance ($\vec{Z}$) of a Li-ion cell in a wide range of frequencies by disturbing the battery with a sinusoidal current (i) and measuring the voltage (v) response or vice versa, as presented in (1).

$$\vec{Z}(j\omega) = \frac{V\sin(\omega t + \phi_v)}{I\sin(\omega t + \phi_i)} = Z_{real} + jZ_{imag} \qquad (1)$$

where ω is the angular velocity of the signal that depends on the excitation frequency, ϕ is their phase, and Z_{real} and Z_{imag} are the real and imaginary parts, respectively, of the complex impedance of the battery.

The result of a frequency sweep is a spectrum of cell complex impedance at various frequencies. To represent this spectrum, a Nyquist plot is commonly used, in which the negative imaginary part of the impedance ($-Z_{imag}$) is plotted against the real part (Z_{real}). Fig. 2 shows a Nyquist plot for a LIB. Three zones are distinguished according to the frequency range. Each zone is dominated by different electrochemical phenomena [18], as can be seen in the figure. While at low and medium frequencies the cell impedance shows a combination of resistive and capacitive effects, at high frequencies it shows

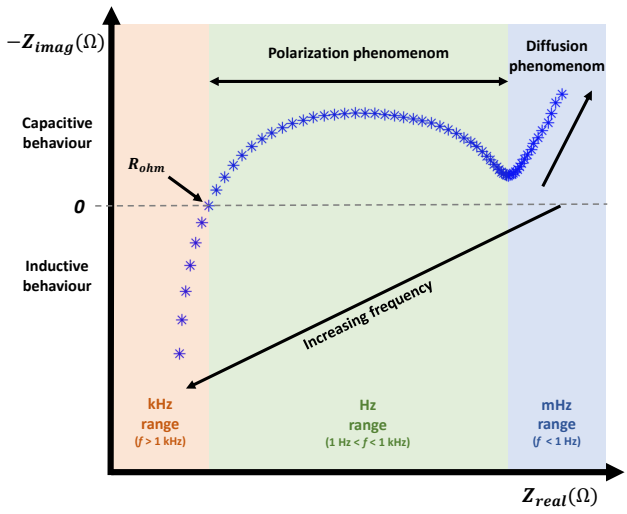

Fig. 2: Main phenomena that can be measured by means of EIS represented in a Nyquist plot, and associated frequencies.

inductive behavior, mainly due to the measuring system and geometry of the cell [19]. When Z_{imag} is zero, the ohmic resistance (R_{ohm}) is defined. R_{ohm} includes the ionic conductivity of the electrolyte as well as the electronic conductivity of electrodes, current collectors and electrical contacts [17].

III. Experimental set-up

A. Investigated cell

A pouch Li-ion/polymer cell, SLPB8643128H5 by Kokam, is analyzed in this study. It has a nominal capacity of 3.6 Ah, a nominal voltage of 3.7 V and a maximum and minimum voltages of 4.2 V and 2.7 V respectively. This cell contains NMC-LCO composite cathode, the anode is composed of carbon/graphite and the electrolyte is based on a solution of lithium hexafluorophosphate ($LiPF_6$) in a mixture of organic solvent ethylene carbonate (EC) and ethyl methyl carbonate (EMC). See other general specifications in Table I.

B. Description of the experiments

Five overtemperature abuse experiments are performed at different SOCs (0, 25, 50, 75 and 100 %). The cell is heated slowly and homogeneously to achieve a uniform temperature distribution throughout the cell. Moreover, due to the small size of the cell, the temperature gradients can be neglected and the surface temperature can be considered to be equal to the internal temperature. The heating method consists of applying progressive temperature steps each 90 minutes. The test starts from laboratory ambient temperature, around 20–25 °C, and the set points for each step are 60 °C, 100 °C, 120 °C and 140 °C. Fig. 3 shows the overtemperature test method. For the last two heating steps, an exothermic behavior of the cell can be observed. During the test, EIS measurements are repeated every five minutes. Each EIS takes about 2.5 minutes. The temperature value associated to each EIS is the average cell temperature during the measurement.

C. Testing equipment

The experiments presented in this contributions are carried out at the Laboratory for Energy Storage and Microgrids of the Public University of Navarre shown in Fig. 4. The abuse experiments are carried out inside an 80 L resistant stainless-steel oven, which can heat the cell up to 220 °C. Five K–type thermocouples measure the cell temperature, while three are used to measure the ambient temperatures at different points inside and outside the oven. Cold-junction compensated

TABLE I: Specifications of the tested Li-ion cell.

Cathode	NMC + LCO
Anode	Graphite
Electrolyte	$LiPF_6$ + EC:EMC
Mean voltage	3.7 V
Nominal capacity	3.6 Ah
AC Impedance (1 kHz)	3 mΩ
Dimensions	129 mm x 43 mm x 8.8 mm
Specific energy	145 Wh/kg

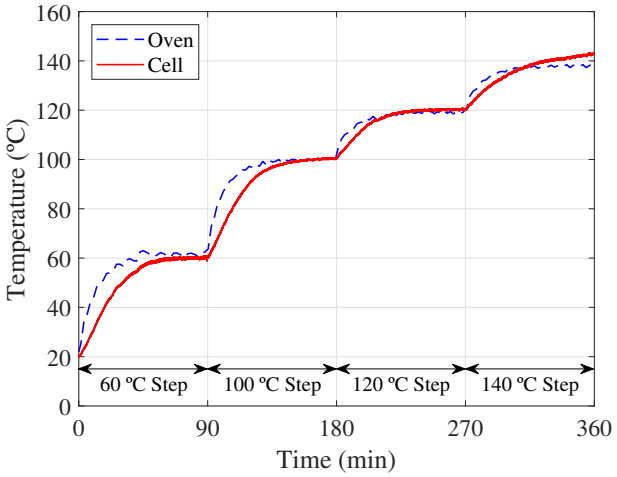

Fig. 3: Overtemperature abuse test procedure.

thermocouple-to-digital converters MAX31855 are used to monitor these temperatures. These devices have an accuracy of ±2 °C for temperatures ranging from –200 °C to 700 °C. A Raspberry Pi 3B+ is used for temperature data acquisition, with a sample rate of 15 Hz. Finally, EIS measurements are carried out using the EVAL-ADICUP3029 circuit board and EVAL-AD5941BATZ battery measurement board, in the range from 1 Hz to 10000 Hz.

IV. Experimental results

Fig. 5 shows the EIS measurements during the overtemperature test on 100 % SOC cell. The cell impedance decreases with increasing temperature for $T < 80$ °C, which has a greater impact at low frequencies. However, a trend change is observed for $T > 90$ °C. From 90 °C to 100 °C, Z_{real} increases progressively while Z_{imag} remains almost constant. Finally, for higher temperatures, both Z_{real} and Z_{imag} increase notably. Furthermore, the impedance shifts to the right at 140 °C, indicating a sudden increase in ohmic impedance, which can be attributed to the separator shutdown [2].

Fig. 4: Experimental test bench in the Laboratory for Energy Storage and Microgrids of the Public University of Navarre.

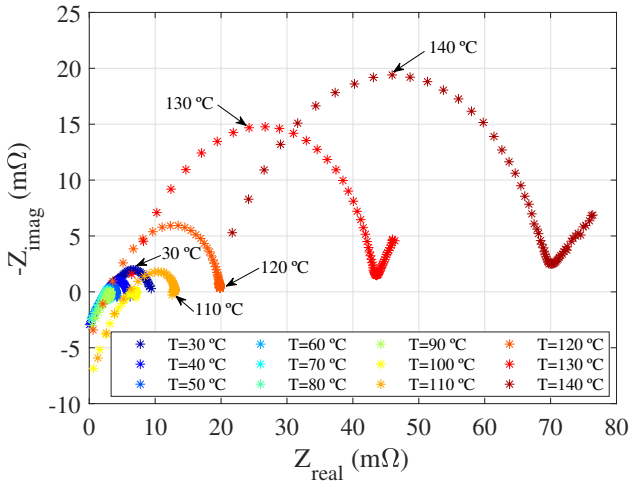

Fig. 5: EIS measurements during the overtemperature test on 100 % SOC cell every 10 °C.

The above-mentioned relationship between temperature and cell impedance (Z_{real} and Z_{imag}) at different frequencies for $SOC = 100$ % are shown in Fig. 6(a) with closer detail. Z_{real} undergoes a progressive reduction at low frequencies as temperature increases from 25 °C to 60 °C, while this decrease is smaller for higher frequencies. However, from 90 °C onward, Z_{real} increases exponentially for all frequencies. On the other hand, Z_{imag} has a similar response, decreasing with increasing temperature from 25 °C to 60 °C, and even changes from capacitive to inductive behavior. From 60 °C to 100 °C, Z_{imag} remains almost constant for all frequencies. Finally, for temperatures above 100 °C, Z_{imag} increases exponentially, with a slope depending on the frequency. The effect of temperature on the phase of the complex impedance (ϕ) is also studied and is depicted in Fig. 6(b). The evolution of ϕ with temperature is considerably different at each frequency and there is no observable progression from low to high frequencies. However, the common trend of ϕ at all frequencies is to increase (decrease for $-\phi$) from 25 °C to 80 °C. From 80 °C, ϕ at 1 and 1000 Hz increases significantly, while the values for 10 and 100 Hz have significantly lower variations.

Therefore, a clear trend change in the cell impedance is observed at temperatures around 80–90 °C. For lower temperatures, Z_{real}, Z_{imag} and $-\phi$ decrease with increasing temperature, as identified in previous literature [12], [14], [16], while the opposite is true at temperatures higher than 90 °C. Sharp increase of Z_{real} and Z_{imag} is obtained from 90 °C and 110 °C, respectively. The reduction in resistance with increasing temperature is mainly due to the reduction in electrolyte viscosity, which improves electrolyte lithium ion conductivity [15]. On the other hand, the increase in impedance at higher temperatures can be attributed to the initiation of degradation reactions or vaporization of the electrolyte, which are reported to occur at temperatures above 90 °C [3]. As a consequence of these phenomena occurring at high temperatures, the impedance increases exponentially.

V. Temperature Estimation and Overtemperature Detection

Based on the experimental results, Z_{real}, Z_{imag} and ϕ are compared to obtain the most reliable variable to estimate Li-ion battery temperature looking for higher accuracy in the overtemperature region. Z_{real} is considered the best option as it is very sensitive to temperatures below 80 °C and its value increases significantly above 90 °C (see Fig. 6(a)), providing a very trustworthy indicator of Li-ion battery overtemperature. By contrast, Z_{imag} is the worst choice, given that its sensitivity at low temperatures is lower and its increase for high temperatures is delayed until 110 °C. Finally, ϕ is very sensitive to low temperatures, as discussed in literature [12], but its response to high temperatures is unpredictable, as shown in Fig. 6(b). Therefore, Z_{real} is proposed as the best indicator for temperature monitoring when overtemperature detection is a desired characteristic.

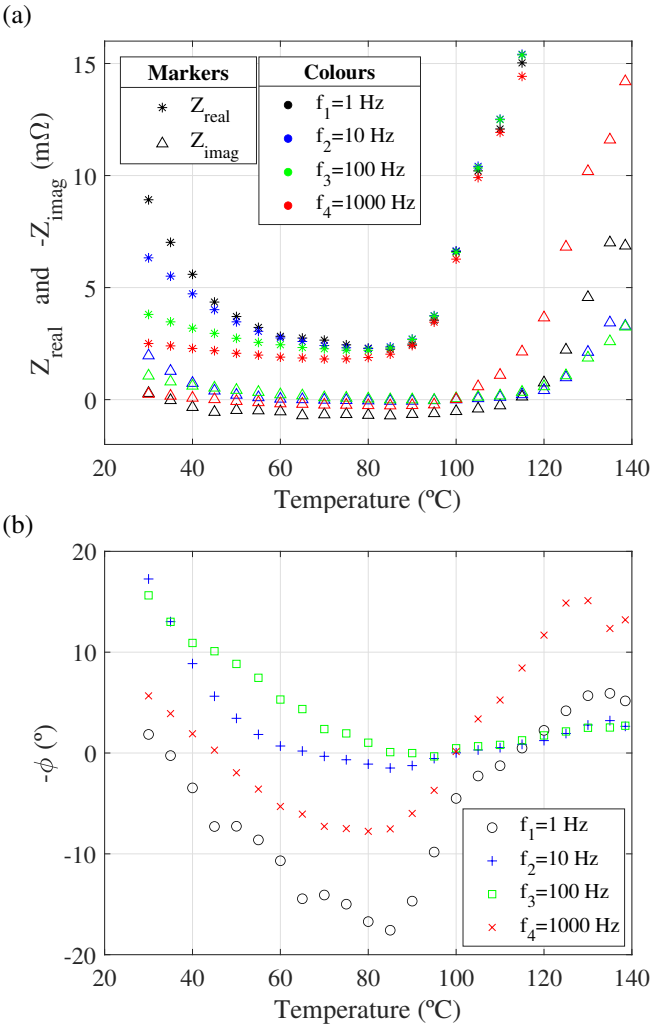

Fig. 6: EIS measurements during the overtemperature test on 100 % SOC cell at 1, 10, 100 and 1000 Hz. a) Z_{real} ("*" symbol) and Z_{imag} ("△" symbol); and b) Phase (ϕ).

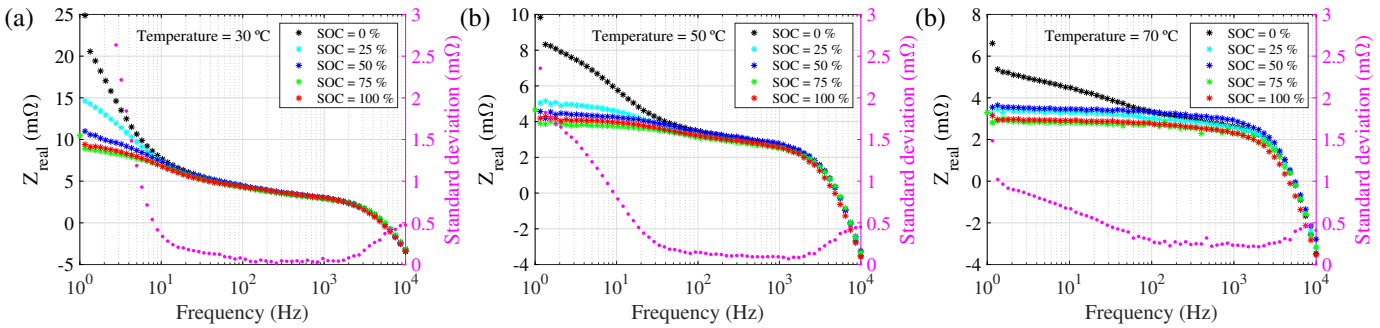

Fig. 7: Z_{real} vs. frequency at various SOCs and temperatures. The standard deviation between the different SOCs is shown in pink. a) Temperature of 30 °C. b) Temperature of 50 °C. c) Temperature of 70 °C.

The application of EIS to detect battery overtemperature in a real application is usually problematic due to the time required to perform the measurement. Once the experimental results of EIS are analyzed, a measurement of the impedance of the cell at a single frequency is proposed in the following lines as a shorter measurement procedure. However, the behavior of the cell impedance with temperature depends on frequency. Moreover, not only the temperature influences the impedance, but also the SOC. For this reason, the selected frequency must satisfy a compromise between high temperature dependency and a low dependency on SOC. In order to analyze the SOC dependency of Z_{real}, the standard deviation (s) is computed. Thus, the dispersion of Z_{real} between five different SOCs is calculated for each frequency using the following expression:

$$s = \sqrt{\frac{\sum_{i=1}^{N}(x_i - \overline{x})^2}{N-1}} \tag{2}$$

where N is the number of different SOCs studied (five in this work), x_i is the Z_{real} value for each SOC at the same frequency and $\overline{x}$ is the mean value for the values of all SOCs at the corresponding frequency.

In Fig. 7 the value of Z_{real} vs. frequency at various SOCs is represented for three different temperatures, with the standard deviation at each frequency marked with pink dots. As can be observed, the influence of the SOC on Z_{real} is greater at low frequencies. As discussed in [14], those low frequencies include the charge transfer process which is highly dependent on the SOC. However, as the frequency increases, the standard deviation decreases significantly, indicating less dispersion and dependence on the SOC. Frequencies between 100 Hz and 2000 Hz satisfy the minimum dependence of the SOC on Z_{real}. However, it should be noted that the higher the frequency, the lower the sensitivity of Z_{real} with temperature, as shown in Fig. 6(a). Taking both considerations into account, a frequency of 100 Hz is selected to achieve adequate temperature dependence and SOC independence.

In order to assess the reliability of the Z_{real} indicator at a frequency of 100 Hz, the low and high temperature ranges are analyzed. In Fig. 8, the Z_{real} values for temperatures below 60 °C are shown. Generally, 60 °C would be the maximum temperature limit set by LIB manufacturers. A linear relationship between Z_{real} and temperature is observed, which improves its estimation. Furthermore, the behavior of Z_{real} for each SOC maintains the same linear relationship with temperature. However, SOC dispersion increases with temperature and could worsen accuracy if it is unknown. Despite this fact, the reliability of temperature estimation by measuring cell impedance is again demonstrated.

Finally, in Fig. 9, the overall response of Z_{real} at 100 Hz for all SOCs and temperatures studied is presented. This graph clearly shows the exponential increase of Z_{real} for temperatures above 100 °C. As can be observed, when the temperature of the cell reaches 100 °C, Z_{real} is equal to its value at 25 °C. Since battery systems always have one or more temperature sensors, there should exist no conflict in estimating the correct temperature above 100 °C based on cell impedance. Furthermore, as Z_{real} increases significantly, the impedance response is a clear indicator of high temperatures in the cell. Therefore, it is proved that Z_{real} is able to detect high temperatures, providing reliable and fast detection.

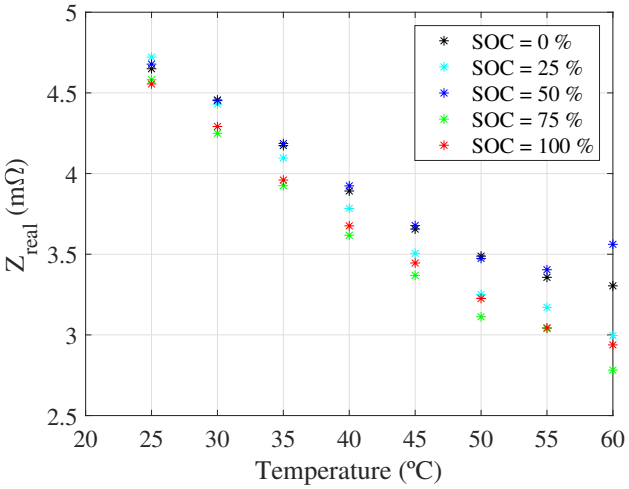

Fig. 8: Z_{real} at 100 Hz and various SOCs for temperatures below 60 °C.

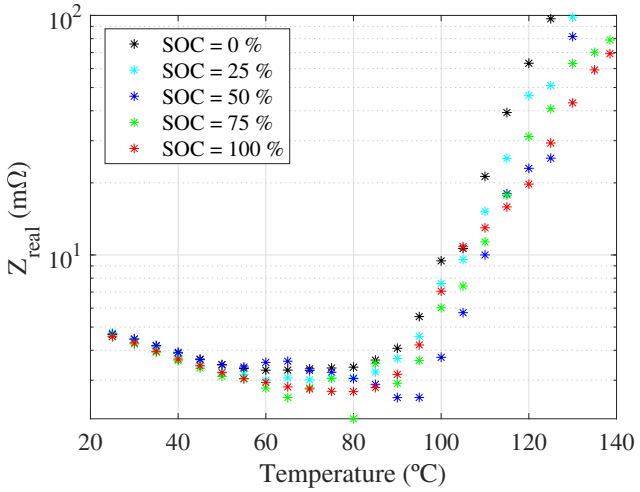

Fig. 9: Z_{real} at 100 Hz and various SOCs for all temperatures analyzed.

VI. Conclusions

The main objective of this work is to highlight the need to monitor the temperature of LIBs, as it is an essential factor affecting their performance, lifetime and safety. Especially relevant is to have a high sensitivity to overtemperature, which can lead to thermal runaway events. Given the cost of assembling temperature sensors in all the cells of a battery pack, EIS is presented as a method capable of estimating the temperature of all the cells of a battery, thus reducing the number of temperature sensors required. EIS has already been identified as a promising tool for monitoring internal battery status (SOC and SOH). Therefore, it can be combined with existing BMSs to enhance their potential and increase the performance and safety of LIBs.

EIS measurements are obtained on a commercial Li-ion battery at different temperatures, from 25 °C to 140 °C, and new findings on temperature estimation are revealed. The influence of temperature on cell impedance is analyzed at various frequencies for different SOCs. Based on these results, Z_{real} is proposed as the best temperature indicator given its high sensitivity to overtemperature events. A simplification of the EIS technique is proposed, selecting a single frequency to estimate the cell temperature, reducing time and complexity of the measurement method. The measurement of Z_{real} at 100 Hz allows an accurate estimation of the temperature under safe conditions and a high sensitivity for temperatures above 100 °C, avoiding the onset of unwanted chemical reactions.

After the laboratory validation presented in this work, the proposed method based on cell impedance as a temperature estimator should be tested in real applications, such as a battery pack under operating conditions. In addition, the influence of non-uniform temperature distribution within the cell or aging on cell impedance must be studied to ensure accurate temperature control throughout the battery lifetime.

References

[1] A. Soto, A. Berrueta, M. Mateos, P. Sanchis, and A. Ursúa, "Impact of micro-cycles on the lifetime of lithium-ion batteries: An experimental study," *Journal of Energy Storage*, vol. 55, p. 105343, 2022.

[2] Y. Chen, Y. Kang, Y. Zhao, L. Wang, J. Liu, Y. Li, Z. Liang, X. He, X. Li, N. Tavajohi, and B. Li, "A review of lithium-ion battery safety concerns: The issues, strategies, and testing standards," *Journal of Energy Chemistry*, vol. 59, pp. 83–99, 2021.

[3] I. Lalinde, A. Berrueta, J. J. Valera, J. Arza, P. Sanchis, and A. Ursúa, "Perspective chapter: Thermal runaway in lithium-ion batteries," in *Lithium-Ion Batteries - Recent Advanced and Emerging Topics*, D. G. Lamblin, Ed. Rijeka: IntechOpen, 2022, ch. 3.

[4] I. Lalinde, A. Berrueta, P. Sanchis, and A. Ursúa, "Applied method to model the thermal runaway of lithium-ion batteries," in *2021 IEEE International Conference on Environment and Electrical Engineering and 2021 IEEE Industrial and Commercial Power Systems Europe (EEEIC/I&CPS Europe)*, 2021, pp. 1–6.

[5] Q. Wang, B. Mao, S. I. Stoliarov, and J. Sun, "A review of lithium ion battery failure mechanisms and fire prevention strategies," *Progress in Energy and Combustion Science*, vol. 73, pp. 95–131, 2019.

[6] L. Lu, X. Han, J. Li, J. Hua, and M. Ouyang, "A review on the key issues for lithium-ion battery management in electric vehicles," *Journal of Power Sources*, vol. 226, pp. 272–288, 2013.

[7] M. Alipour, C. Ziebert, F. V. Conte, and R. Kizilel, "A review on temperature-dependent electrochemical properties, aging, and performance of lithium-ion cells," *Batteries*, vol. 6, no. 3, 2020.

[8] T. Grandjean, A. Barai, E. Hosseinzadeh, Y. Guo, A. McGordon, and J. Marco, "Large format lithium ion pouch cell full thermal characterisation for improved electric vehicle thermal management," *Journal of Power Sources*, vol. 359, pp. 215–225, 2017.

[9] Y. Zhang, Q. Tang, Y. Zhang, J. Wang, U. Stimming, and A. A. Lee, "Identifying degradation patterns of lithium ion batteries from impedance spectroscopy using machine learning," *Nature Communications*, vol. 11, 2020.

[10] J. Kim and J. Kowal, "Development of a matlab/simulink model for monitoring cell state-of-health and state-of-charge via impedance of lithium-ion battery cells," *Batteries*, vol. 8, no. 2, 2022.

[11] M. Kuipers, P. Schröer, T. Nemeth, H. Zappen, A. Blömeke, and D. U. Sauer, "An algorithm for an online electrochemical impedance spectroscopy and battery parameter estimation: Development, verification and validation," *Journal of Energy Storage*, vol. 30, p. 101517, 2020.

[12] R. Srinivasan, B. G. Carkhuff, M. H. Butler, and A. C. Baisden, "Instantaneous measurement of the internal temperature in lithium-ion rechargeable cells," *Electrochimica Acta*, vol. 56, no. 17, pp. 6198–6204, 2011.

[13] R. Srinivasan, P. A. Demirev, and B. G. Carkhuff, "Rapid monitoring of impedance phase shifts in lithium-ion batteries for hazard prevention," *Journal of Power Sources*, vol. 405, pp. 30–36, 2018.

[14] J. P. Schmidt, S. Arnold, A. Loges, D. Werner, T. Wetzel, and E. Ivers-Tiffée, "Measurement of the internal cell temperature via impedance: Evaluation and application of a new method," *Journal of Power Sources*, vol. 243, pp. 110–117, 2013.

[15] J. Zhu, Z. Sun, X. Wei, and H. Dai, "A new lithium-ion battery internal temperature on-line estimate method based on electrochemical impedance spectroscopy measurement," *Journal of Power Sources*, vol. 274, pp. 990–1004, 2015.

[16] H. Zappen, G. Fuchs, A. Gitis, and D. U. Sauer, "In-operando impedance spectroscopy and ultrasonic measurements during high-temperature abuse experiments on lithium-ion batteries," *Batteries*, vol. 6, no. 2, 2020.

[17] N. Meddings, M. Heinrich, F. Overney, J.-S. Lee, V. Ruiz, E. Napolitano, S. Seitz, G. Hinds, R. Raccichini, M. Gaberšček, and J. Park, "Application of electrochemical impedance spectroscopy to commercial li-ion cells: A review," *Journal of Power Sources*, vol. 480, p. 228742, 2020.

[18] A. Soto, A. Berrueta, I. Oficialdegui, P. Sanchis, and A. Ursúa, "Noninvasive aging analysis of lithium-ion batteries in extreme cold temperatures," *IEEE Transactions on Industry Applications*, vol. 58, no. 2, pp. 2400–2410, 2022.

[19] C. Fleischer, W. Waag, H.-M. Heyn, and D. U. Sauer, "On-line adaptive battery impedance parameter and state estimation considering physical principles in reduced order equivalent circuit battery models: Part 1. requirements, critical review of methods and modeling," *Journal of Power Sources*, vol. 260, pp. 276–291, 2014.